Cancer Research

Decoy Receptor DcR1 Is Induced in a p50/Bcl3–Dependent Manner and Attenuates the Efficacy of Temozolomide

Nassir M. Mansour[1], Giovanna M. Bernal[1], Longtao Wu[1], Clayton D. Crawley[1], Kirk E. Cahill[1], David J. Voce[1], Irina V. Balyasnikova[1], Wei Zhang[2], Ruben Spretz[3], Luis Nunez[3], Gustavo F. Larsen[3], Ralph R. Weichselbaum[4], and Bakhtiar Yamini[1]

Abstract

Temozolomide is used widely to treat malignant glioma, but the overall response to this agent is generally poor. Resistance to DNA-damaging drugs such as temozolomide has been related to the induction of antiapoptotic proteins. Specifically, the transcription factor NF-κB has been suggested to participate in promoting the survival of cells exposed to chemotherapy. To identify factors that modulate cytotoxicity in the setting of DNA damage, we used an unbiased strategy to examine the NF-κB–dependent expression profile induced by temozolomide. By this route, we defined the decoy receptor DcR1 as a temozolomide response gene induced by a mechanism relying upon p50/NF-κB1. A conserved NF-κB–binding sequence (κB-site) was identified in the proximal promoter and was demonstrated to be required for DcR1 induction by temozolomide. Loss-of-function and gain-of-function studies reveal that the atypical IκB protein, Bcl3, is also required for induction of DcR1 by temozolomide. Mechanistically, DcR1 attenuates temozolomide efficacy by blunting activation of the Fas receptor pathway in $p53^{+/+}$ glioma cells. Intracranial xenograft studies show that DcR1 depletion in glioma cells enhances the efficacy of temozolomide. Taken together, our results show how DcR1 upregulation mediates temozolomide resistance and provide a rationale for DcR1 targeting as a strategy to sensitize gliomas to this widely used chemotherapy. *Cancer Res; 75(10); 2039–48. ©2015 AACR.*

Introduction

Over the past decade, the oral alkylating agent temozolomide has become the standard chemotherapeutic for the management of malignant glioma. Specifically, the addition of temozolomide to ionizing radiation improves overall patient survival by approximately 2 months (1). Despite the clinical success of temozolomide, it is clear that many patients respond poorly to this agent at least in part due to the intrinsic resistance of tumor cells to damage-induced cell death. Temozolomide causes cytotoxicity by forming O^6-methylguanine (O^6-MeG) adducts that mismatch with deoxythymidine residues and induce apoptosis following processing by the mismatch repair system (2). Although the repair protein O^6-methylguanine DNA methyltransferase (MGMT) plays a prominent role in resistance to temozolomide (3, 4), downstream factors that regulate induction of apoptosis are also important in the overall response.

NF-κB is a pivotal factor in the cytotoxic response to DNA damage (5). Although DNA double-strand breaks activate NF-κB by a well-elucidated nuclear to the cytoplasmic pathway (6), temozolomide and other replication stress-inducing agents modulate NF-κB signaling in a more complex, promoter-specific manner (7–9). The NF-κB family of proteins is comprised of five subunits: p50 (NF-κB1, p105), p52 (NF-κB2, p100), p65 (relA), relB, and crel that appear in their mature form as dimers (10). In general, NF-κB dimers are retained in the cytoplasm through interaction with the inhibitor-κB (IκB) proteins and, following translocation to the nucleus, mediate their effect by binding to specific consensus elements (κB-sites) in the promoter regions of genes. Although all NF-κB subunits contain a conserved N-terminal rel homology domain, only p65, relB and crel have a C-terminal transactivation domain (TAD). p50 is a ubiquitously expressed NF-κB subunit that is targeted by the temozolomide-induced DNA damage response (8). Despite the lack of a TAD, p50 can induce NF-κB–dependent gene expression by associating with other rel subunits or coregulator proteins. Bcl3 is one such NF-κB coregulator that was originally identified at the t(14;19) chromosomal translocation in chronic lymphocytic leukemia patients (11, 12). Bcl3 was subsequently found to be an atypical IκB protein that modulates NF-κB transcriptional activity in conjunction with p50- or p52-containing dimers (13). In this capacity, Bcl3 has been reported to induce the expression of antiapoptotic factors such as Bcl2 or Hdm2 (14, 15).

Apoptosis in response to temozolomide is reported to involve both the intrinsic, or mitochondrial, pathway and the extrinsic, or

[1]Department of Surgery, Section of Neurosurgery, The University of Chicago, Chicago, Illinois. [2]College of Medicine, The University of Illinois at Chicago, Chicago, Illinois. [3]LNK Chemsolutions LLC, Lincoln, Nebraska. [4]Department of Radiation and Cellular Oncology and The Ludwig Center for Metastasis Research, The University of Chicago, Chicago, Illinois.

Note: Supplementary data for this article are available at Cancer Research Online (http://cancerres.aacrjournals.org/).

N.M. Mansour and G.M. Bernal contributed equally to this article.

Corresponding Author: Bakhtiar Yamini, University of Chicago, 5841 South Maryland Avenue, Chicago, IL 60637. Phone: 773-702-8544; Fax: 773-702-3518; E-mail: byamini@surgery.bsd.uchicago.edu

doi: 10.1158/0008-5472.CAN-14-2144

receptor-induced, response (16, 17). The extrinsic pathway is initiated by receptor–ligand binding, resulting in caspase-mediated cell death (18). TNF receptor superfamily members such as Fas receptor (Fas, CD95, and Apo-1) and TNF-related apoptosis-inducing ligand-receptor 1 (TRAIL-R1, DR4) or TRAIL-R2 (DR5) mediate killing via the extrinsic response. In addition to these death receptors, two decoy receptors, DcR1 (TRAIL-R3, TRID, and TNFRSF10C) and DcR2 (TRAIL-R4 and TRUNDD), have been described previously. Decoy receptors do not induce cell death as they lack critical components that are necessary for apoptosis signaling (19). DcR1, a model decoy receptor, is found preferentially in untransformed cells (20) and attenuates apoptosis by competing with DR4 and DR5 or by forming an inactive heteromer with other death receptors (21). DcR1, like other TRAIL receptors, is a p53 target gene with an intronic p53-binding site (BS) that is induced by DNA damaging agents (22).

In this study, using an unbiased genome-wide expression analysis, we identify DcR1 as a factor significantly induced by temozolomide in a p50-dependent fashion. Mechanistic studies demonstrate that DcR1 is coregulated by p50 and Bcl3 via a novel κB-site, and *in vitro* and animal studies demonstrate that depletion of DcR1 sensitizes gliomas to cytotoxicity by temozolomide. Together, these findings support the observation that temozolomide induces apoptosis via the death receptor pathway and suggest that targeting DcR1 is a strategy that can potentially enhance the antiglioma effect of temozolomide clinically.

Materials and Methods

Cell lines, reagents, and plasmids

Human U87, A172, T98, and U251 glioblastoma cells were purchased from the ATCC and authenticated by routine morphologic and growth analysis and also by Western blotting. Cells were cultured as previously described (8). U87 glioma cells expressing sh-p105 or sh-control were also previously described (8). pCMV-p50 was previously described (8), and used for experiments in Fig. 4. HA-p50 was cloned from the template, p50 cFlag pcDNA3 (Addgene plasmid 20018), obtained from Dr. Stephen Smale (Department of Microbiology, Immunology, and Molecular Genetics, University of California, Los Angeles, Los Angeles CA), following excision of the Flag and insertion of an HA tag. The Bcl3 expression construct, Bcl3-pFlag-CMV2, was a kind gift from Dr. Albert Baldwin (Department of Biology, University of North Carolina at Chapel Hill, Chapel Hill, NC).

RNA interference and stable transfectants

The following siRNA constructs were obtained from Dharmacon: siGENOME Human Bcl3, si-p53 (M-3329-03), si-DcR1 (sc-40235), and si-scrambled control (D-001210-03-05). Also, si-p50 (sense: GUCACUCUAACGUAUGCAAUU) and si-control (sense: CCUACGCCACCAAUUUCGUUU) were obtained from Santa Cruz Biotechnology. All siRNA constructs were transfected using Oligofectamine (Invitrogen).

To make cells stably expressing sh-DcR1, PAGE-purified oligos (sense: GATCCGCTGAAGAGACAATGAACATTCAAGAGATGTTCATTGTCTCTTCAGCTTTTTTACGCGTG and antisense: ATTCACGCGTAAAAAAGCTGAAGAGACAATGAACATCTCTTGAATGTTCATTGTCTCTTCAGCG) or scrambled control, were obtained from IDT and annealed. Oligos were ligated into the BamHI and EcoRI sites of the retrovirus: pSIREN-RetroQ-DsRed (Clontech). For retroviral production, sh-control and sh-DcR1 vectors were cotransfected with pCMV-VSV-G into Plat-GP cells using Xtreme gene according to the manufacturer's protocol (Roche). After 48 hours, the supernatant was cleared using a 0.45-μm syringe and concentrated using Clontech Retro-X at 3.5 mL per 1 mL of viral supernatant. The virus was collected by centrifugation at 1,500 × *g* for 45 minutes. The pellet was resuspended in regular media with 20 μL polybrene and added to U87 cells. Cells were split after 48 hours and maintained in regular media. Eighty percent to 90% infection efficiency was determined by expression of Ds-Red, and knockdown of DcR1 verified by mRNA and protein analysis.

Immunoblot and electrophoretic mobility shift assay

Immunoblotting was performed using whole-cell lysate as previously described (23). Primary antibodies used include: anti-Bcl3 (Santa Cruz Biotechnology; sc185), anti-p21 (Santa Cruz Biotechnology; sc397), anti-p50 (Santa Cruz Biotechnology; sc7178), anti-GAPDH (Santa Cruz Biotechnology; sc-137179), anti-p53 (Santa Cruz Biotechnology; sc71818), anti-DcR1 (R&D Systems; 398600), and anti-HA (Covance; MMS-101R). Alexa-Fluor 680 and Alexa-Fluor 800 fluorescent dye-conjugated secondary antibodies (Invitrogen) were used for visualization with Odyssey Infrared system (LICOR Biosciences). Electrophoretic mobility shift assay (EMSA) was performed as previously described (8) with competition using cold specific and nonspecific probes and supershift with anti-p50. The κB probe sequence is shown in Fig. 4.

Quantitative real-time PCR and quantitative chromatin immunoprecipitation

Quantitative real-time PCR (qPCR) was performed following total mRNA isolation as described previously (8). *DCR1* was normalized to *GAPDH*, and relative *DCR1* mRNA expression is shown as the average of three experiments performed in triplicate. Primers used for *DCR1* are: sense, CACCAACGCTTCCAACAATGAACC and antisense, TCCGGAAGGTGCCTTCTTTACACT.

Quantitative chromatin immunoprecipitation (qChIP) was also performed as described previously (8) following immunoprecipitation with anti-p50 or anti-Bcl3 antibodies. Control immunoprecipitation was performed using anti-Histone H1 and anti-mouse IgG. qPCR was performed using promoter-specific primers for human DcR1 that span the region encompassing the putative κB-site (sense, CCTCGACCATGCAAAGGGT and antisense, ACAGAATGAAGGACACAGGGG), and the change in DNA enrichment for each immunoprecipitated condition determined relative to input DNA. To control for nonspecific binding, the anti-p50 or anti-Bcl3 data were subtracted from the anti-H1 results (anti-IgG showed no binding) as previously described (8). The PCR product was also run on a gel for a semiquantitative analysis of the data.

Flow cytometric analysis of apoptosis and DcR1 expression

Analysis of apoptosis was performed as described previously (24) at 72 or 96 hours following treatment. For DcR1 surface expression, cells were treated with temozolomide and trypsinized, washed with blocking buffer (PBS + 1% BSA), and centrifuged at 1,500 RPM. The cell pellet was divided into two groups and incubated with anti-DcR1 (Abcam), or anti-IgG control. Pellets were incubated with Alexa-fluor–conjugated secondary antibody and analyzed on an LSRII Flow Cytometer (BD Biosciences). Samples were run in triplicate and data analyzed using FlowJo (TreeStar Inc.).

Luciferase reporter and luciferase assay

For construction of a DcR1 luciferase reporter, we amplified a segment of DNA containing the *DCR1* proximal promoter and

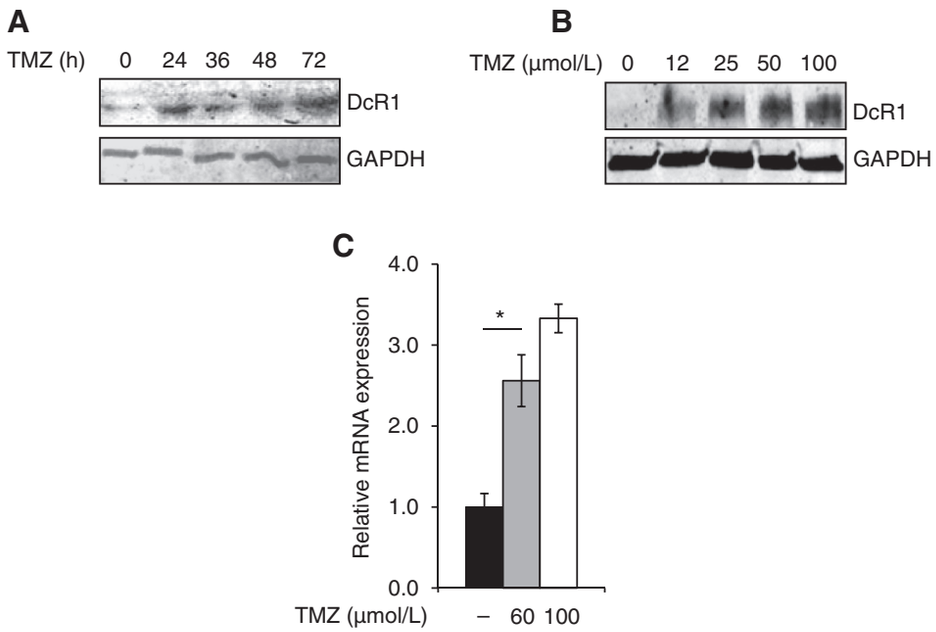

Figure 1.
Temozolomide induces DcR1 expression. A, immunoblot with anti-DcR1 or anti-GAPDH antibody in U87 glioma cells at the indicated time following treatment with 100 μmol/L temozolomide (TMZ). B, immunoblot with anti-DcR1 48 hours following treatment with temozolomide. C, qPCR analysis of *DCR1* mRNA expression in U87 cells 16 hours following treatment with indicated concentration of temozolomide. Data, mean *DCR1* transcript expression relative to *GAPDH* ± SD of triplicate samples from three separate biologic experiments; *, $P < 0.05$.

part of intron 1 using fresh human genomic DNA with the following primers: GATAGACACTTGACTGGGGGAC and GAAGAACTGGGTC. After cloning the 1.232 kbp segment into the pCR II Topo Vector (Invitrogen), the *DCR1* sequence was liberated using XhoI and HindIII and ligated into the pGl4.20 luciferase vector. Site-directed mutagenesis, using the QuickChange Lightning II Mutagenesis Kit, was used to mutate the κB and p53 BSs to the sequences indicated in Fig. 4.

For luciferase assay, cells were cotransfected with the indicated reporter and *Renilla reniformis* and relative luciferase calculated after treatment with temozolomide as described previously (23). All experiments were performed in triplicate.

DcR1 cDNA cloning and lentiviral infection

The coding region of *TNFRSF10C* (NM_003841) was amplified (sense: AGCAGGCTCCGAATTCGCCACCATGGCCCGGATCCCCAAGACCCTA and antisense: AAGCTGGGTCGAATTCTCAAGCGTAATCTGGAACATCGTATGGG TAAACAAACACAATCAGAAGCACAATTAG) using genomic DNA from HEK293T cells. An HA tag was added to the C-terminus for immunoblot detection. This cDNA was then inserted into the pLVX-Puro vector (Clontech) and lentivirus generated using the packaging system from Addgene (pMD2.G and psPAX). U87 cells were then infected with HA-DcR1 lentivirus and selected with puromycin for 5 days.

Clonogenic and Trypan blue assays

Assays were performed essentially as described previously (8, 24). FAS-neutralizing antibody (FNAb) was obtained from Millipore (#05-338). For clonogenic assay with FNAb, U87 cells were transfected with *DCR1*, or control, siRNA and after 48 hours replated. Cells were then treated with 25 μmol/L temozolomide and 1 μg/mL FNAb (or vehicle). FNAb was readministered once 16 hours later and colony number counted at 2 weeks. Data show the change in surviving fraction in temozolomide-treated samples in the presence and absence of FNAb in cells expressing the different siRNAs. Experiment was performed in triplicate and repeated. Clonogenic assay was performed after treatment of U87 cells with 30 ng/mL FAS ligand in the presence and absence of FNAb.

Nanoparticle production and characterization

Nanoparticles (NP) were manufactured and characterized as previously described (25) by LNK Chemsolutions LLC. SiRNA constructs were incorporated into nanoparticles in a similar fashion to incorporation of other agents (25), and the product maintained in sterile conditions.

Animal studies

Six- to 7-week-old male nude mice (Harlan) were used in accordance with guidelines of the Institutional Animal Care and Use Committee of the University of Chicago. For intracranial studies, 5×10^5 U87 cells were injected into the right striatum as previously described (24), and the animals randomized into 6 groups ($n = 6$ per group). Either PBS or nanoparticles (10 μL) carrying si-Control or si-DcR1 were injected intracranially on days 4 and 7 following tumor inoculation. Mice were also treated with i.p. injection of vehicle or temozolomide on days 4 (5 mg/kg), 7 (5 mg/kg), and 10 (2.5 mg/kg; total temozolomide dose: 12.5 mg/kg). Animals were followed until terminal, sacrificed and brains harvested for verification of tumor.

For hindlimb studies, 7.5×10^6 U87 cells were injected into the right hind limb and animals randomized into 6 groups ($n = 5$/group) when tumors reached an average of 120 mm^3 (day 0). Mice were treated with daily i.t. injection of 50 μL nanoparticles containing either si-control or si-DcR1 for 5 consecutive days, and/or i.p. temozolomide (total dose: 12.5 mg/kg). Control animals were injected i.t. or i.p. with vehicle. Tumor volume was measured and documented every 2–3 days.

Statistical analyses

Results are expressed as mean ± SD and significance determined as a P value of <0.05 using a two-tailed Student t test.

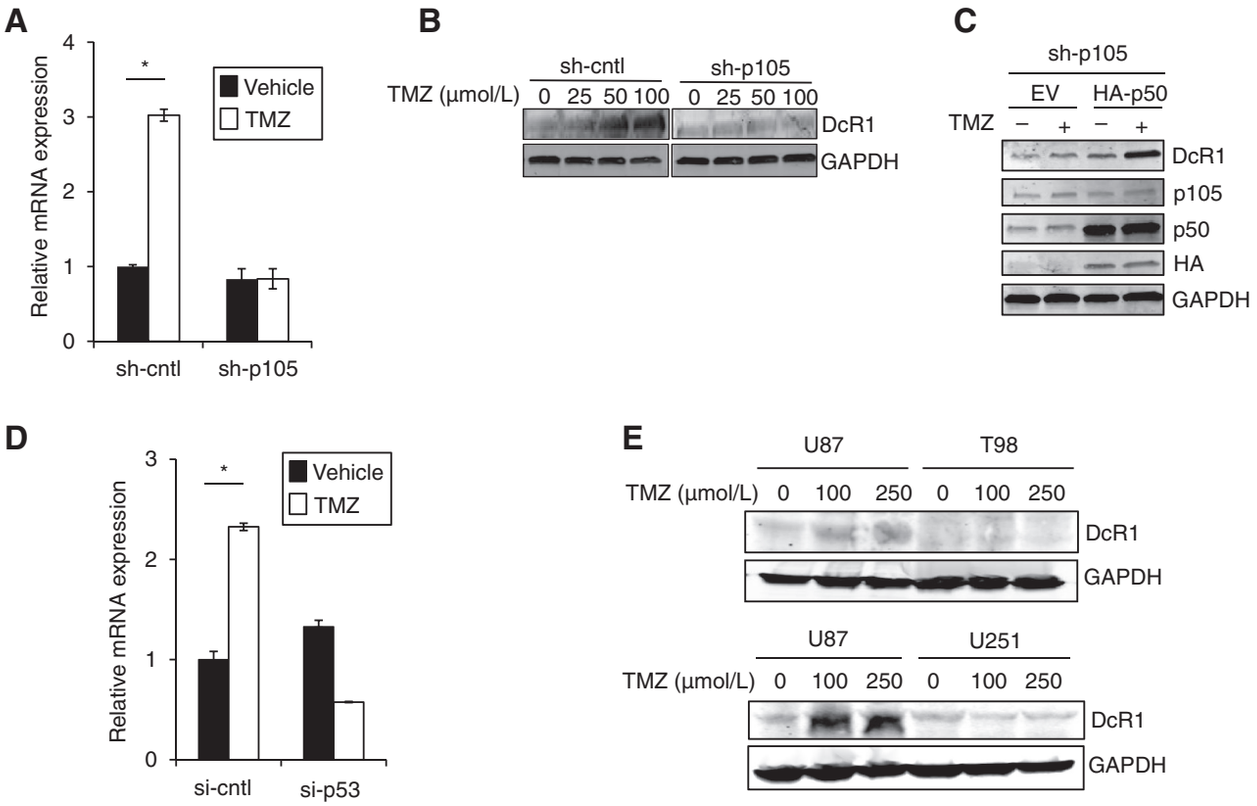

Figure 2.
DcR1 is induced by temozolomide in a p50- and p53-codependent manner. A, qPCR analysis of *DCR1* mRNA expression relative to *GAPDH*, ±SD from triplicate samples from three experiments using U87 cells stably expressing sh-control (cntl) or sh-p105, 16 hours after treatment with vehicle or 100 μmol/L temozolomide (TMZ). B, immunoblot with anti-DcR1 or anti-GAPDH in cells from A, 48 hours following treatment with vehicle or temozolomide. C, immunoblot with the indicated antibody in U87-sh-p105 cells transfected with HA-p50 or empty vector (EV) following treatment with vehicle or 250 μmol/L temozolomide (24 hours). D, qPCR analysis of *DCR1* mRNA expression in U87 cells transfected with si-RNA following treatment with vehicle or 100 μmol/L temozolomide (16 hours). E, immunoblot with anti-DcR1 following treatment of the indicated glioma cell lines with temozolomide for 48 hours; *, $P < 0.05$.

Results

Temozolomide induces DcR1 protein expression

To identify NF-κB–dependent factors that modulate the response to temozolomide, we performed an unbiased genome-wide expression analysis in isogenic glioma cells following treatment with temozolomide. U87 cells stably expressing sh-p105 or sh-control, described previously (8), were treated with temozolomide or vehicle and mRNA expression analyzed using the affymetrix Human Genome U133 Plus 2.0 Array. The expression data will be described in detail in a separate publication (D. Voce; unpublished data). *DCR1* (*TNFRSF10C*) was identified as one of a small set of genes significantly induced only in p50-proficient cells following treatment (Supplementary Fig. S1A). Given the importance of DcR1 in attenuating death receptor-induced apoptosis, we examined this decoy receptor in the response to temozolomide. DcR1 is induced within 24 hours in U87 cells (Fig. 1A), and the induction occurs in a concentration-dependent manner (Fig. 1B). As DcR1 is a cell surface receptor, the change in DcR1 expression was quantified using flow cytometry and, consistent with the immunoblot analysis, DcR1 surface expression is induced by temozolomide (Supplementary Fig. S1B). In addition, temozolomide induces expression of *DCR1* mRNA (Fig. 1C). These results indicate that temozolomide upregulates DcR1 in glioma cells.

DcR1 is induced in a p50- and p53-codependent manner

To verify the p50 dependence of DcR1, U87 cells expressing sh-p105 or sh-control were used. Consistent with the array findings, loss of p105/p50 blocks induction of DcR1 at the mRNA (Fig. 2A) and protein level (Fig. 2B). Moreover, knockdown of p105 also attenuates DcR1 surface expression (Supplementary Fig. S1C). Importantly, reexpression of p50 in sh-p105 cells enables DcR1 induction, confirming that it is p50, and not p105, that is necessary for temozolomide-induced expression of DcR1 (Fig. 2C). Of note, reexpression of p50 is possible because the sh-p105 targets the C-terminus of p105 (8). DcR1 is also a p53 target gene (22), and temozolomide increases expression of p53, and its downstream target p21, with a time course consistent with activation of DcR1 (Supplementary Fig. S1D). Knockdown of p53 blocks the ability of temozolomide to induce *DCR1* mRNA in U87 cells (Fig. 2D). In addition, consistent with p53 dependence, temozolomide does not induce DcR1 in either T98 or U251 glioma cells, both of which are p53 mutant, even at a concentration of 250 μmol/L (Fig. 2E). These results indicate that DcR1 is

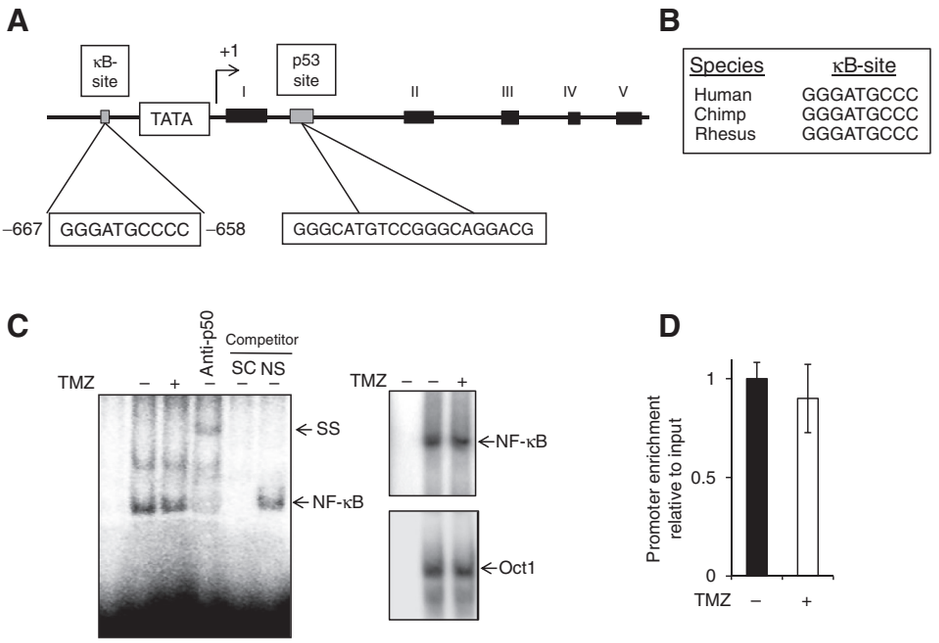

Figure 3.
DCR1 contains a conserved κB-site that binds p50. A, schematic representation of *DCR1* showing the putative κB-site and p53 BS. B, conservation of *DCR1* κB-site sequence in primates. C, EMSA with the DcR1 κB-site probe using nuclear extract from U87 cells treated with vehicle or 100 μmol/L temozolomide (TMZ; 16 hours). Competition with specific and nonspecific competitors (SC and NS), respectively. Supershift (SS) was performed using anti-p50. Oct1 EMSA (right) demonstrates equal lysate loading. D, qChIP using *DCR1* promoter-specific primers spanning the putative κB-site. Data, chromatin enrichment of p50 relative to input after controlling for nonspecific binding using anti-histone H1 (positive control) and anti-IgG, normalized to vehicle, ±SD of three triplicate samples, repeated with similar results.

induced by temozolomide in a p50-dependent manner and also verify the importance of p53 in regulating DNA damage-induced DcR1.

DcR1 contains a conserved κB-site that binds p50

As our data indicate that DcR1 is transcriptionally regulated by NF-κB, we therefore searched the promoter and first intron of *DCR1* (NCBI Gene ID: 8794) for potential NF-κB consensus elements. Using the program, TFSEARCH (26), a 10-nucleotide sequence sharing 86% homology with the canonical κB-site was identified in the *DCR1* proximal promoter (Fig. 3A). *DCR1* has only been described in primates (NCBI search *TNFRSF10C*), and an identical nucleotide sequence is found in other primate species (Fig. 3B). Gel shift assay (EMSA) shows that the putative κB-site binds NF-κB *in vitro* and supershift analysis demonstrates that p50 is present within the NF-κB band (Fig. 3C). Also, temozolomide does not alter the binding of NF-κB to the κB-site (Fig. 3C). To examine whether p50 binds the *DCR1* promoter *in vivo*, ChIP assay was performed. p50 is recruited to the region of the *DCR1* promoter containing the κB-site, and consistent with the EMSA, temozolomide does not significantly change this (Fig. 3D). A blot of the PCR product further verifies the enrichment of p50 in this region (Supplementary Fig. S2A, right).

To examine the functional significance of this consensus site, we constructed a luciferase reporter bearing a 1.232 kbp region encompassing the proximal promoter, exon 1 and a segment of the first intron of *DCR1* (Fig. 4A). Given information from previous DcR1 promoter/reporters (22, 27), our reporter was constructed to contain the p53 BS shown to be important for DcR1 induction. Temozolomide induces expression from this reporter that peaks at 12 hours (Fig. 4B). Mutation of the p53 BS or κB-site blocks basal and induced reporter activity (Fig. 4C) demonstrating that the putative κB-site is necessary for activity of the reporter. We next examined whether this site is regulated by p50. Knockdown of p105/p50 blocks induction of activity from the wild-type (wt) reporter in response to temozolomide (Fig. 4D). Moreover, when p50 is reexpressed in sh-p105 cells, a substantial increase in basal activity is seen that is further increased by temozolomide (Fig. 4D, right). These results suggest that a κB-site in the *DCR1* promoter binds p50 and is required for p50-mediated induction by temozolomide.

Induction of DcR1 by temozolomide requires Bcl3

Despite the p50/p53 codependence of DcR1, in A172 cells that are p53-wt (28) and have abundant p50, temozolomide only slightly induces expression of DcR1 (Fig. 5A). To further study this observation, we looked at the cytogenetics of A172 cells and noted that these cells have a significant deletion near chromosome 19q13.2 (29), a region containing the locus of the NF-κB coregulator, *BCL3*. As Bcl3 plays a prominent role in p50-dependent gene activation (30), we investigated whether DcR1 requires Bcl3 for induction by temozolomide. First, it is evident that, although A172 cells do express Bcl3, they have substantially less than some other glioma cell lines (Fig. 5B). Also, in U87 cells ChIP assay confirms that Bcl3 is bound to the *DCR1* promoter and its recruitment minimally altered by treatment (Supplementary Fig. S2A). Knockdown of Bcl3 completely blocks the ability of temozolomide to induce *DCR1* mRNA (Fig. 5C) and protein expression (Fig. 5D). Moreover, depletion of Bcl3 blocks the ability of temozolomide to induce activation of the *DCR1* promoter/intron 1 reporter (Fig. 5E). To confirm the role of Bcl3, we obtained a Bcl3 cDNA construct (gift from Dr. Albert Baldwin). Overexpression of Bcl3 in A172 cells enables temozolomide to induce DcR1 expression (Fig. 5F), an observation also noted in U87 cells (Supplementary Fig. S2B). Together, these data indicate that temozolomide requires Bcl3 to induce DcR1 expression.

Induction of DcR1 blocks the cytotoxic effect of temozolomide

DcR1 attenuates apoptosis (21), suggesting that its induction by temozolomide acts to block killing. Depletion of DcR1 leads to

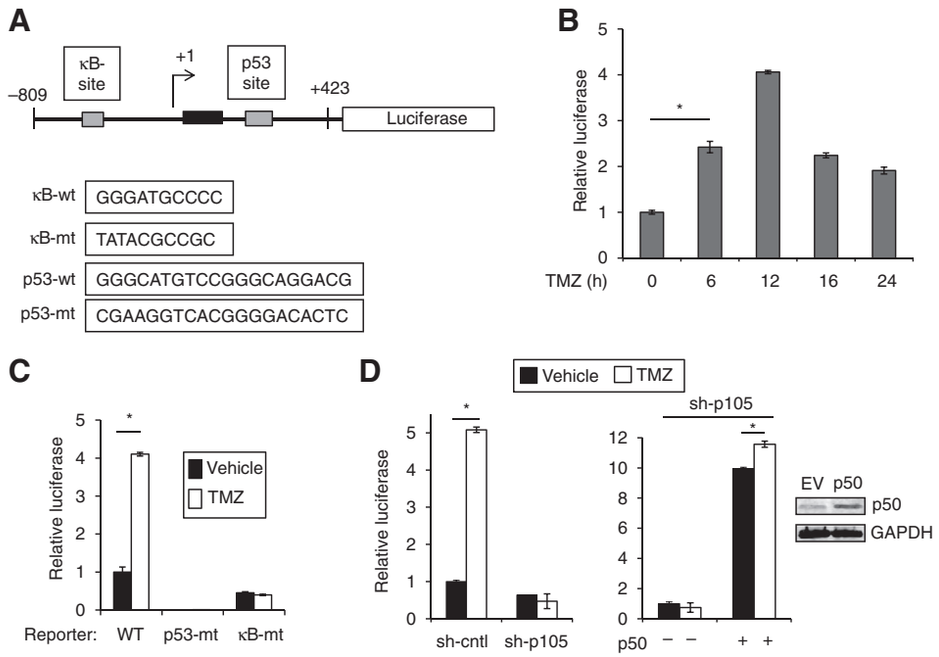

Figure 4.
The κB-site and p50 are required for activation of a *DCR1* promoter/intron 1 reporter by temozolomide. A, schematic representation of the 1.232 kbp luciferase reporter. B, luciferase expression relative to *Renilla* in U87 cells using the wt-reporter following treatment with 100 μmol/L temozolomide (TMZ) for the indicated time. C, relative luciferase activity from the indicated reporter following treatment of U87 cells with vehicle or 100 μmol/L temozolomide (12 hours). D, relative luciferase in sh-p105 and sh-control cells (left), and in sh-p105 cells transfected with empty vector (EV) or p50 (right) following treatment as in C. Inset, immunoblot with anti-p50 antibody. Luciferase data represent mean ±SD of triplicate samples; *, $P < 0.01$.

a significant increase in apoptosis following temozolomide treatment as assessed by annexin V binding ($P < 0.05$, Fig. 6A). As a specificity control, we also constructed U87 cell lines expressing shRNAs targeting *DcR1* or a scrambled sequence. Three DcR1 shRNA constructs were used and cell lines screened for knockdown of DcR1 using qPCR (Supplementary Fig. S2C). Cells expressing sh-DcR1-3 were selected and depletion of DcR1 protein confirmed by immunoblot analysis (Fig. 6B, inset). Sh-RNA depletion of DcR1 augments induction of apoptosis by temozolomide (Fig. 6B) supporting the siRNA data and confirming that the effect is not due to the specific siRNA used. In addition, as temozolomide induces cytotoxicity at late times following treatment, we examined cell viability over time using Trypan blue dye exclusion. Temozolomide increases the percentage of nonviable cells over time and knockdown of DcR1 augments this effect beginning 72 hours after treatment (Supplementary Fig. S2D). As DcR1 is not induced by temozolomide in U251 cells, we also examined cytotoxicity in these cells. Knockdown of DcR1 does not affect induction of apoptosis by temozolomide in U251 cells (Supplementary Fig. S3A).

We next examined clonal survival. Depletion of DcR1 augments the decrease in survival induced by temozolomide in U87 cells (Fig. 6C) and to a lesser extent in A172 cells (Supplementary Fig. S3B), likely due to the lower level of DcR1 induction in A172 cells compared with U87 cells. By contrast, in U251 cells no significant change in clonal survival is seen in response to temozolomide following DcR1 depletion compared with control (Supplementary Fig. S3C). To further study the importance of DcR1, we cloned a cDNA of human HA-tagged DcR1 and constructed an HA-DcR1 lentiviral expression vector. U87 cells were infected with this construct and stable expression of HA-DcR1 confirmed by immunoblot analysis (Fig. 6D). Overexpression of DcR1 significantly attenuates the decrease in clonal survival induced by temozolomide relative to vector control (Fig. 6D). Taken together, overexpression and downregulation studies indicate that DcR1 acts to attenuate the anti-glioma effect of temozolomide.

Given that DcR1 specifically blocks death receptor-induced cytotoxicity, we sought to examine whether DcR1 affects the temozolomide-induced death receptor response. It was previously noted that induction of apoptosis by temozolomide is attenuated by an FNAb that blocks death receptor signaling (17). We used FNAb in temozolomide-treated U87 cells that were initially transfected with siRNA targeting either DcR1 or a control sequence. Although exposure to FNAb results in a 1.2-fold increase in clonal survival in temozolomide-treated cells expressing si-control, in cells depleted of DcR1 there is almost a 4-fold increase in survival in the presence of FNAb (Fig. 6E). The observation that blocking the death receptor response with FNAb has a more profound effect in the presence of DcR1 knockdown, suggests that DcR1 inhibits apoptosis induced by temozolomide specifically by affecting the death receptor pathway. Importantly, we verified that in our hands FNAb does attenuate the decrease in survival induced by Fas ligand (FasL; Supplementary Fig. S4A). Moreover, although FNAb does not directly bind DcR1, both FNAb and DcR1 modulate apoptosis via the same receptor-mediated downstream signaling cascade (31). Consistent with DcR1 playing a role in the Fas response, whereas knockdown of DcR1 augments the effect of FasL (Supplementary Fig. S4B), overexpression of DcR1 completely blocks the effect of FasL (Supplementary Fig. S4C). Of note, depletion of DcR1 has much less profound effect than DcR1 overexpression likely because of the low basal DcR1 level. In sum, these findings indicate that induction of DcR1 blocks death receptor–mediated cytotoxicity in response to temozolomide.

Knockdown of DcR1 enhances the effect of temozolomide in a glioma model

We next sought to examine DcR1 depletion in an animal glioma model. As there are no DcR1 inhibitors, blocking this factor requires a genetic approach. Stable sh-DcR1 cells do not form xenografts, therefore, we targeted DcR1 by encapsulating

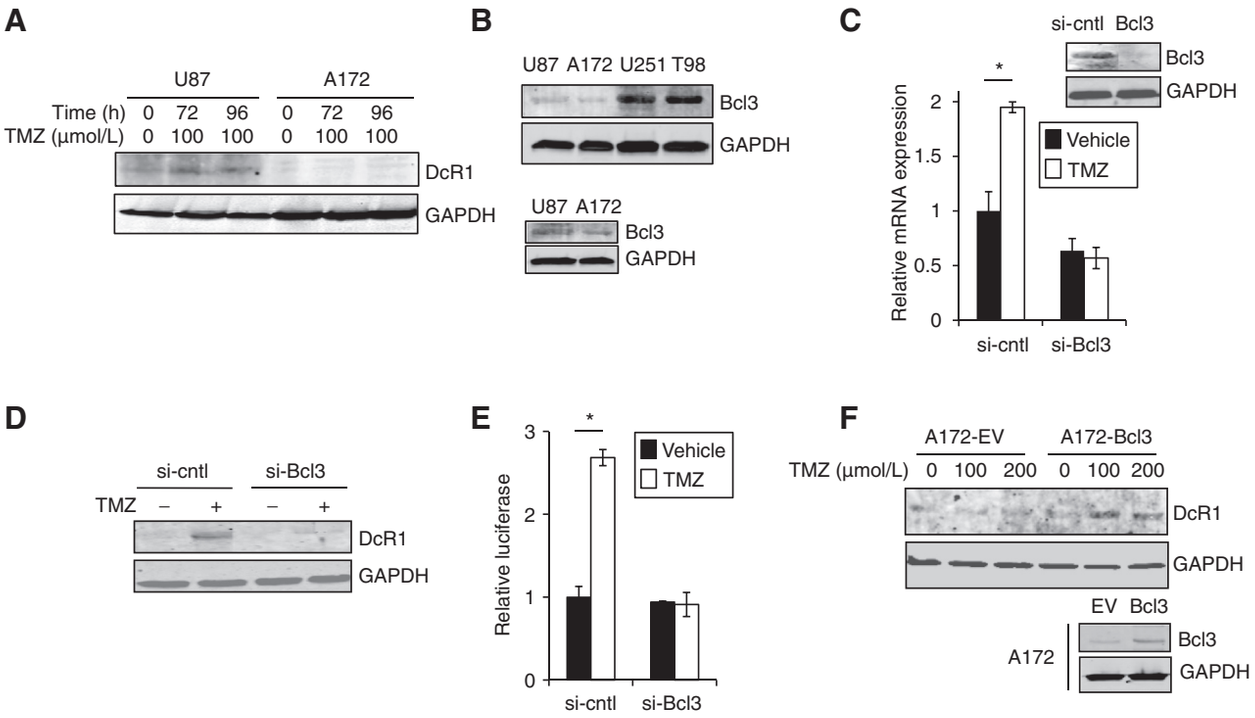

Figure 5.
Bcl3 is required for induction of DcR1 by temozolomide. A, immunoblot with anti-DcR1 in U87 and A172 cells following treatment with temozolomide (TMZ). B, top, immunoblot with anti-Bcl3 antibody using the indicated glioma cells (40-μg protein). Bottom, U87 and A172 cells using 80-μg protein. C, qPCR analysis of mean *DCR1* mRNA expression relative to *GAPDH*, ±SD of triplicate samples in U87 cells transfected with siRNA following treatment (temozolomide: 100 μmol/L). Inset, immunoblot with anti-Bcl3. D, immunoblot with anti-DcR1 in cells transfected and treated as in C. E, relative luciferase expression following treatment with vehicle or 100 μmol/L temozolomide (16 hours) using the wt reporter in cells transfected as in C, mean ±SD of triplicate samples shown. F, immunoblot at 48 hours with anti-DcR1 (top) or anti-Bcl3 (bottom) antibody in A172 cells transfected with empty vector (EV) or Bcl3 and treated as shown; *, $P < 0.05$.

and delivering siRNA using a biodegradable nanoparticle vector previously described for the treatment of malignant glioma (25). Nanoparticles were fabricated to encapsulate either DcR1 siRNA (NP-si-DcR1) or control siRNA (NP-si-cntl). Exposure of U87 cells to NP-si-DcR1 results in a decrease in DcR1 protein expression relative to vehicle or NP-si-cntl (Fig. 7A). In addition, NP-si-DcR1 results in a significant decrease in clonal survival in combination with temozolomide relative to that with temozolomide and NP-si-cntl (Fig. 7B). To examine efficacy *in vivo*, intracranial U87 glioma xenografts were established and nanoparticles administered by direct intracranial injection. A significant increase in animal survival is seen in mice treated with combination temozolomide and NP-si-DcR1 compared with either agent alone or to the combination of temozolomide and NP-si-cntl ($P < 0.01$, log-rank: temozolomide + NP-si-DcR1 vs. temozolomide + NP-si-cntl; Fig. 7C). A similar finding is also seen when hindlimb xenografts are treated with temozolomide and nanoparticles ($P < 0.01$, temozolomide + NP-si-DcR1 vs. NP-si-DcR1; Supplementary Fig. S4D). These findings indicate that in an established growing intracranial xenograft, depletion of DcR1 combines effectively with temozolomide to improve the anti-glioma effect.

Discussion

NF-κB plays a central role in regulating the cytotoxic response to DNA damage. To identify potential factors that modulate the cytotoxic effect of temozolomide, we examined the NF-κB–dependent expression profile induced by this agent in glioma cells. *DCR1*, a decoy receptor that attenuates death receptor–induced apoptosis, was identified as an NF-κB/p50–dependent gene significantly induced by treatment. Given that death receptor signaling is important for temozolomide-induced apoptosis (17), we examined the role of DcR1 in the response to temozolomide. Our findings demonstrate that DcR1 is induced by temozolomide in a manner dependent not only on p50 and p53, but also on the proto-oncogene, Bcl3. Moreover, we show that DcR1 attenuates the cytotoxic effect of temozolomide. In support of the ability of DcR1 to attenuate the anti-glioma response, examination of the Repository for Molecular Brain Neoplasia Data database indicates that patients with upregulated *DCR1* expression do significantly worse than others (Supplementary Fig. S5; ref. 32).

Although it has previously been reported that DNA damage can induce DcR1 and that this response attenuates sensitivity to TRAIL (33), upregulation of DcR1 has not previously been reported to directly block DNA damage–induced killing. In demonstrating that inhibition of DcR1 augments killing by temozolomide, our data support the hypothesis that temozolomide induces cytotoxicity, at least in part, via the death receptor pathway (17). This hypothesis is further suggested by the finding that FNAb has a greater inhibitory effect on the temozolomide-induced response (i.e., causes a greater increase in survival) when DcR1 is depleted than when DcR1 is present.

The NF-κB dependence of DcR1 is supported by identification of a conserved κB-site within the proximal promoter of the *DCR1*

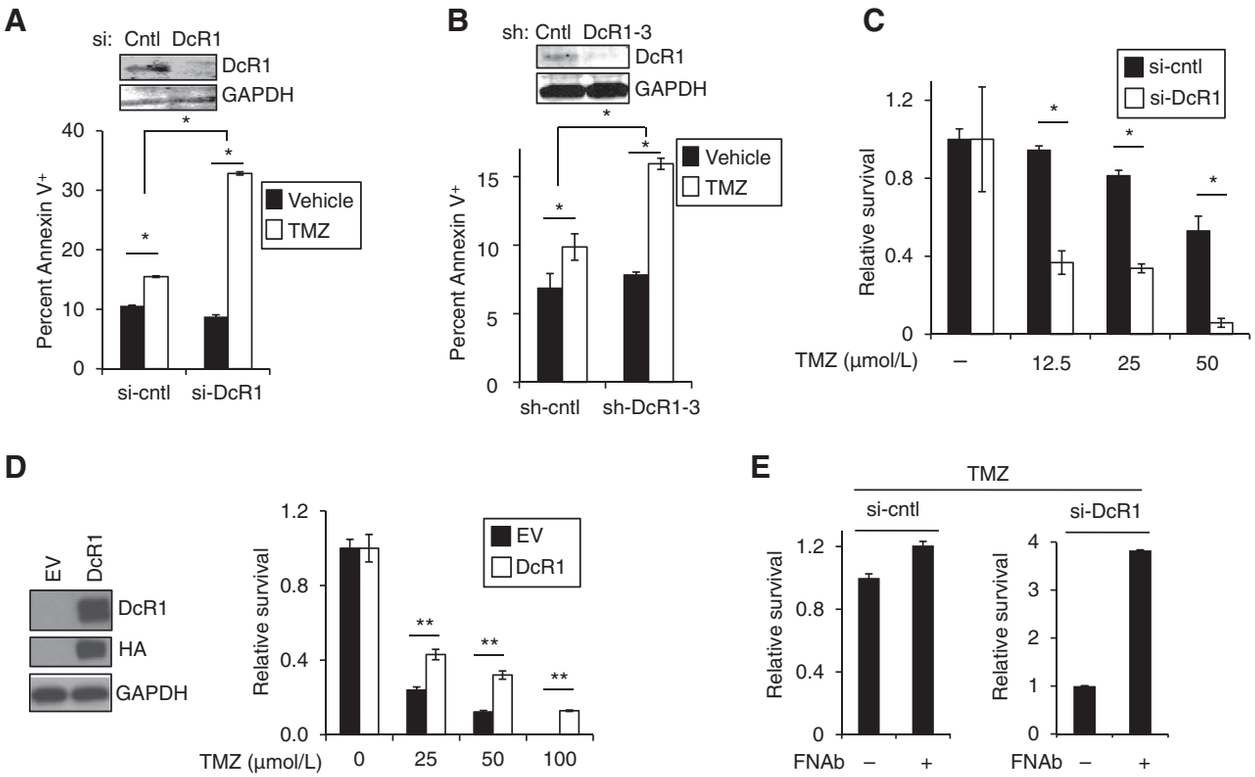

Figure 6.

Depletion of DcR1 sensitizes cells to temozolomide. A, Annexin V binding in U87 cells treated as shown [temozolomide (TMZ): 100 μmol/L, 72 hours] following transfection with the indicated siRNA. B, Annexin V binding at 96 hours in U87 shRNA clones treated as shown (temozolomide: 100 μmol/L). Inset, immunoblot with anti-DcR1. C, clonogenic assay in U87 cells transfected with the indicated siRNA and treated with temozolomide. D, clonogenic assay in U87 clones expressing HA-DcR1 or empty vector (EV) following treatment with temozolomide. Inset, immunoblot with anti-DcR1 or anti-HA. E, clonogenic assay in U87 cells transfected with the indicated siRNA, treated with 25 μmol/L temozolomide and 1 μg/mL FNAb (twice) or vehicle. Data, survival following temozolomide treatment in samples treated with FNAb relative to those without FNAb in each siRNA group. All data represent mean ±SD of triplicate samples, repeated with similar findings; *, $P < 0.05$; **, $P < 0.01$.

gene. p50 binds this κB-site *in vitro* and is also recruited to the promoter region containing this sequence *in vivo*. Moreover, this consensus element is necessary for activation of a DcR1 promoter/reporter by temozolomide. Together, these findings support a functional role for the κB-site in regulating DcR1 expression in response to temozolomide. It is notable that the putative *DCR1* κB-site contains a conserved deoxythymidine (T) residue at the −1 position. Interestingly, we previously reported that phosphorylation of p50 by temozolomide results in inhibition of NF-κB binding to κB-sites with a −1C or G, while binding to κB-sites with a −1A or −1T is unaltered (9). Consistent with this observation, p50 binding to the *DCR1* κB-site (5′-GGGATGCCCC-3′) is unchanged following temozolomide treatment. In addition, the NF-κB dependence of DcR1 is also consistent with a previous study that noted that this gene is induced by crel and blocked by IκBα, respectively (34). Although a specific κB-site has not previously been reported for *DCR1*, functional consensus sequences have been identified for both *DR4* and *DR5* (35, 36), death receptors that are highly homologous to *DCR1* (31).

DcR1 is induced in a p50-dependent manner; however, this NF-κB subunit lacks a TAD and requires either a rel subunit or additional factor to induce NF-κB–dependent gene expression. The atypical IκB protein, Bcl3, is an important NF-κB coregulator that contains two TADs and has been shown to induce NF-κB–dependent gene expression in conjunction with DNA bound p50 (30). We demonstrate that Bcl3 is necessary for efficient DcR1 expression in response to temozolomide. In support of this hypothesis, although loss of Bcl3 in U87 cells blocks the ability of temozolomide to induce DcR1, Bcl3 overexpression has the opposite effect, enhancing DcR1 induction. In addition, the findings that Bcl3 binds the *DCR1* promoter *in vivo* and that Bcl3 depletion blocks temozolomide-induced expression from the *DCR1* promoter/reporter support the hypothesis that this coregulator directly modulates the expression of DcR1. From a mechanistic perspective, given the minimal change in p50 and Bcl3 recruitment to the *DCR1* promoter following treatment (Fig. 3D and Supplementary Fig. S2A), it is likely that temozolomide promotes DcR1 expression by inducing NF-κB posttranslational modifications and/or by inducing recruitment of additional p50- or Bcl3-dependent cofactors (37).

DcR1, like its counterpart DcR2, was initially identified as a receptor preferentially expressed in normal tissues relative to cancer cells (20, 38). However, it is evident that even in cancer cells DcR1 expression is inducible and attenuates DNA damage-induced cytotoxicity. Similarly, DcR2 is also induced by chemotherapeutics in malignant cells (39). These observations raise the possibility that targeting decoy receptors is a strategy that can potentially enhance the therapeutic effect of DNA-damaging

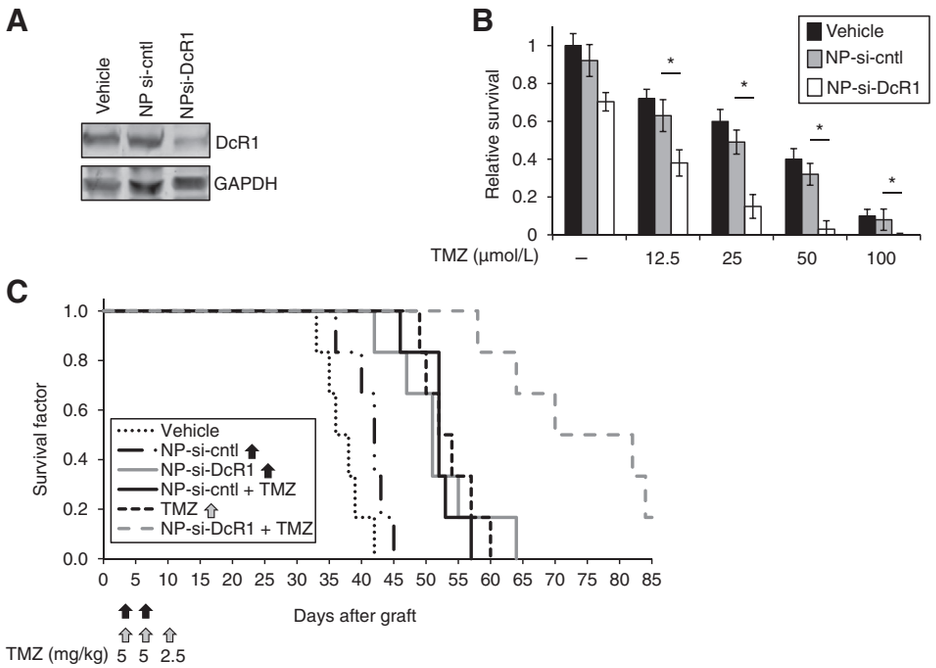

Figure 7.
Knockdown of DcR1 enhances the anti-glioma effect of temozolomide. A, immunoblot with anti-DcR1 antibody in U87 cells treated with vehicle or nanoparticles carrying the indicated siRNA. B, clonogenic assay in U87 cells treated with vehicle or the indicated nanoparticle and temozolomide (TMZ); *, $P < 0.05$. C, Kaplan–Meier survival curves of mice bearing intracranial gliomas ($n = 6$ mice/group) following treatment with temozolomide (days 4, 7, and 10) at the concentrations indicated, and/or nanoparticles carrying the indicated siRNA; $P < 0.01$, log-rank: temozolomide + NP-si-DcR1 versus NP-si-DcR1 or temozolomide + NP-si-cntl.

agents. Consistent with this hypothesis, we demonstrate that depletion of DcR1 enhances the cytotoxic effect of temozolomide. Moreover, by targeting DcR1 in an animal glioma model, we show that blocking expression of this receptor enhances the overall anti-glioma effect. Importantly, the *in vivo* effect of blocking DcR1 is demonstrated against a growing intracranial tumor whose cells were not previously manipulated to deplete DcR1, this finding highlights the potential of DcR1 as a viable clinical chemosensitizing target.

Despite the efficacy of RNAi for targeted depletion of proteins, *in vivo* knockdown of genes is hampered by various factors that include among other things, the protection of the siRNA and efficient delivery to the target tissue (40). To improve these aspects, we encapsulated the DcR1 siRNA in a biocompatible nanoparticle vector that directly delivers its payload to the cytoplasm (25). In addition, nanoparticles were injected directly into the brain to concentrate delivery to the tumor cells. Although siRNA-mediated DcR1 depletion is good for proof-of-principle studies in an animal model, ultimately, delivery of a pharmacologic inhibitor may be a more effective strategy for clinical use.

Inhibition of cellular resistance pathways is an effective strategy to enhance the therapeutic effect of cytotoxic agents. Although blocking NF-κB can improve the antitumor effect of certain chemotherapeutics (41), this transcription factor has a variable role in cytotoxic signaling and is often required for cell death (8, 42). Nevertheless, NF-κB promotes expression of many antiapoptotic factors, suggesting that selective targeting of downstream NF-κB–dependent genes is a strategy that can be used to rationally enhance cytotoxicity. Although temozolomide induces cell death primarily via the intrinsic apoptotic response in p53 mutant gliomas, in p53 wt tumors the exogenous pathway predominates (17). DcR1 represents an anti-apoptotic factor robustly induced by temozolomide that attenuates killing in p53-wt tumors. Given that virtually every patient diagnosed with malignant glioma is treated with temozolomide, targeting factors such as DcR1 can potentially make a significant impact on patient management specifically in tumors that are wt for p53.

Disclosure of Potential Conflicts of Interest

R. Spretz, L. Nunez, and G.F. Larsen have ownership interest (including patents) in LNK Chemsolutions LLC. No potential conflicts of interest were disclosed by the other authors.

Authors' Contributions

Conception and design: B. Yamini

Development of methodology: N.M. Mansour, L. Wu, C.D. Crawley, K.E. Cahill, D.J. Voce, R. Spretz, L. Nunez

Acquisition of data (provided animals, acquired and managed patients, provided facilities, etc.): N.M. Mansour, G.M. Bernal, L. Wu, C.D. Crawley, K.E. Cahill, D.J. Voce, I.V. Balyasnikova

Analysis and interpretation of data (e.g., statistical analysis, biostatistics, computational analysis): N.M. Mansour, G.M. Bernal, L. Wu, C.D. Crawley, K.E. Cahill, D.J. Voce, W. Zhang, L. Nunez, R.R. Weichselbaum, B. Yamini

Writing, review, and/or revision of the manuscript: N.M. Mansour, G.M. Bernal, D.J. Voce, W. Zhang, R. Spretz, L. Nunez, G.F. Larsen, R.R. Weichselbaum, B. Yamini

Administrative, technical, or material support (i.e., reporting or organizing data, constructing databases): N.M. Mansour, G.M. Bernal, C.D. Crawley, G.F. Larsen

Study supervision: B. Yamini

Other (designed nanoparticles): R. Spretz, G.F. Larsen

Grant Support

This work was supported by 1R01CA136937 (B. Yamini), the Ludwig Center for Metastasis Research, and R44CA135906 (R. Spretz, L. Nunez, and B. Yamini).

The costs of publication of this article were defrayed in part by the payment of page charges. This article must therefore be hereby marked *advertisement* in accordance with 18 U.S.C. Section 1734 solely to indicate this fact.

Received July 23, 2014; revised January 15, 2015; accepted February 12, 2015; published OnlineFirst March 25, 2015.

References

1. Stupp R, Mason WP, van den Bent MJ, Weller M, Fisher B, Taphoorn MJ, et al. Radiotherapy plus concomitant and adjuvant temozolomide for glioblastoma. N Engl J Med 2005;352:987–96.
2. Newlands ES, Stevens MF, Wedge SR, Wheelhouse RT, Brock C. Temozolomide: a review of its discovery, chemical properties, pre-clinical development, and clinical trials. Cancer Treat Rev 1997;23:35–61.
3. Kaina B, Fritz G, Mitra S, Coquerelle T. Transfection and expression of human O6-methylguanine-DNA methyltransferase (MGMT) cDNA in Chinese hamster cells: the role of MGMT in protection against the genotoxic effects of alkylating agents. Carcinogenesis 1991;12:1857–67.
4. Hegi ME, Diserens AC, Gorlia T, Hamou MF, de Tribolet N, Weller M, et al. MGMT gene silencing and benefit from temozolomide in glioblastoma. N Engl J Med 2005;352:997–1003.
5. Janssens S, Tschopp J. Signals from within: the DNA-damage-induced NF-kappaB response. Cell Death Differ 2006;13:773–84.
6. Wu ZH, Shi Y, Tibbetts RS, Miyamoto S. Molecular linkage between the kinase ATM and NF-kappaB signaling in response to genotoxic stimuli. Science 2006;311:1141–6.
7. Perkins ND. Post-translational modifications regulating the activity and function of the nuclear factor kappa B pathway. Oncogene 2006;25:6717–30.
8. Schmitt AM, Crawley CD, Kang S, Raleigh DR, Yu X, Wahlstrom JS, et al. p50 (NF-kappaB1) is an effector protein in the cytotoxic response to DNA methylation damage. Mol Cell 2011;44:785–96.
9. Crawley CD, Raleigh DR, Kang S, Voce DJ, Schmitt AM, Weichselbaum RR, et al. DNA damage-induced cytotoxicity is mediated by the cooperative interaction of phospho-NF-kappaB p50 and a single nucleotide in the kappaB-site. Nucleic Acids Res 2012;41:764–74.
10. Ghosh S, Hayden MS. New regulators of NF-kappaB in inflammation. Nat Rev Immunol 2008;8:837–48.
11. Wulczyn FG, Naumann M, Scheidereit C. Candidate proto-oncogene bcl-3 encodes a subunit-specific inhibitor of transcription factor NF-kappa B. Nature 1992;358:597–9.
12. Crossen PE. Cytogenetic and molecular changes in chronic B-cell leukemia. Cancer Genet Cytogenet 1989;43:143–50.
13. Palmer S, Chen YH. Bcl-3, a multifaceted modulator of NF-kappaB-mediated gene transcription. Immunol Res 2008;42:210–8.
14. Viatour P, Merville MP, Bours V, Chariot A. Protein phosphorylation as a key mechanism for the regulation of BCL-3 activity. Cell Cycle 2004;3:1498–501.
15. Kashatus D, Cogswell P, Baldwin AS. Expression of the Bcl-3 proto-oncogene suppresses p53 activation. Genes Dev 2006;20:225–35.
16. Hickman MJ, Samson LD. Apoptotic signaling in response to a single type of DNA lesion, O(6)-methylguanine. Mol Cell 2004;14:105–16.
17. Roos WP, Batista LF, Naumann SC, Wick W, Weller M, Menck CF, et al. Apoptosis in malignant glioma cells triggered by the temozolomide-induced DNA lesion O6-methylguanine. Oncogene 2007;26:186–97.
18. Fulda S, Debatin KM. Extrinsic versus intrinsic apoptosis pathways in anticancer chemotherapy. Oncogene 2006;25:4798–811.
19. Yerbes R, Palacios C, Lopez-Rivas A. The therapeutic potential of TRAIL receptor signalling in cancer cells. Clin Transl Oncol 2011;13:839–47.
20. Pan G, Ni J, Wei YF, Yu G, Gentz R, Dixit VM. An antagonist decoy receptor and a death domain-containing receptor for TRAIL. Science 1997;277:815–8.
21. Ashkenazi A, Dixit VM. Apoptosis control by death and decoy receptors. Curr Opin Cell Biol 1999;11:255–60.
22. Ruiz de Almodovar C, Ruiz-Ruiz C, Rodriguez A, Ortiz-Ferron G, Redondo JM, Lopez-Rivas A. Tumor necrosis factor-related apoptosis-inducing ligand (TRAIL) decoy receptor TRAIL-R3 is up-regulated by p53 in breast tumor cells through a mechanism involving an intronic p53-binding site. J Biol Chem 2004;279:4093–101.
23. Yamini B, Yu X, Dolan ME, Wu MH, Darga TE, Kufe DW, et al. Inhibition of nuclear factor-kappaB activity by temozolomide involves O6-methylguanine induced inhibition of p65 DNA binding. Cancer Res 2007;67:6889–98.
24. Yamini B, Yu X, Gillespie GY, Kufe DW, Weichselbaum RR. Transcriptional targeting of adenovirally delivered tumor necrosis factor alpha by temozolomide in experimental glioblastoma. Cancer Res 2004;64:6381–4.
25. Bernal GM, Lariviere MJ, Mansour N, Pytel P, Cahill KE, Voce DJ, et al. Convection-enhanced delivery and *in vivo* imaging of polymeric nanoparticles for the treatment of malignant glioma. Nanomedicine 2014;10:149–57.
26. Heinemeyer T, Wingender E, Reuter I, Hermjakob H, Kel AE, Kel OV, et al. Databases on transcriptional regulation: TRANSFAC, TRRD and COMPEL. Nucleic Acids Res 1998;26:362–7.
27. Ruiz de Almodovar C, Lopez-Rivas A, Redondo JM, Rodriguez A. Transcription initiation sites and promoter structure of the human TRAIL-R3 gene. FEBS Lett 2002;531:304–8.
28. Wischhusen J, Naumann U, Ohgaki H, Rastinejad F, Weller M. CP-31398, a novel p53-stabilizing agent, induces p53-dependent and p53-independent glioma cell death. Oncogene 2003;22:8233–45.
29. Law ME, Templeton KL, Kitange G, Smith J, Misra A, Feuerstein BG, et al. Molecular cytogenetic analysis of chromosomes 1 and 19 in glioma cell lines. Cancer Genet Cytogenet 2005;160:1–14.
30. Fujita T, Nolan GP, Liou HC, Scott ML, Baltimore D. The candidate proto-oncogene bcl-3 encodes a transcriptional coactivator that activates through NF-kappa B p50 homodimers. Genes Dev 1993;7:1354–63.
31. Sheikh MS, Fornace AJ Jr. Death and decoy receptors and p53-mediated apoptosis. Leukemia 2000;14:1509–13.
32. National Cancer Institute. 2005. REMBRANDT home page. Accessed 2012 June 18. Available from: http://rembrandt.nci.nih.gov.
33. Toscano F, Fajoui ZE, Gay F, Lalaoui N, Parmentier B, Chayvialle JA, et al. P53-mediated upregulation of DcR1 impairs oxaliplatin/TRAIL-induced synergistic anti-tumour potential in colon cancer cells. Oncogene 2008;27:4161–71.
34. Bernard D, Quatannens B, Vandenbunder B, Abbadie C. Rel/NF-kappaB transcription factors protect against tumor necrosis factor (TNF)-related apoptosis-inducing ligand (TRAIL)-induced apoptosis by up-regulating the TRAIL decoy receptor DcR1. J Biol Chem 2001;276:27322–8.
35. Mendoza FJ, Ishdorj G, Hu X, Gibson SB. Death receptor-4 (DR4) expression is regulated by transcription factor NF-kappaB in response to etoposide treatment. Apoptosis 2008;13:756–70.
36. Shetty S, Graham BA, Brown JG, Hu X, Vegh-Yarema N, Harding G, et al. Transcription factor NF-kappaB differentially regulates death receptor 5 expression involving histone deacetylase 1. Mol Cell Biol 2005;25:5404–16.
37. Baek SH, Ohgi KA, Rose DW, Koo EH, Glass CK, Rosenfeld MG. Exchange of N-CoR corepressor and Tip60 coactivator complexes links gene expression by NF-kappaB and beta-amyloid precursor protein. Cell 2002;110:55–67.
38. Sheridan JP, Marsters SA, Pitti RM, Gurney A, Skubatch M, Baldwin D, et al. Control of TRAIL-induced apoptosis by a family of signaling and decoy receptors. Science 1997;277:818–21.
39. Liu X, Yue P, Khuri FR, Sun SY. Decoy receptor 2 (DcR2) is a p53 target gene and regulates chemosensitivity. Cancer Res 2005;65:9169–75.
40. Tiemann K, Rossi JJ. RNAi-based therapeutics-current status, challenges and prospects. EMBO Mol Med 2009;1:142–51.
41. Wang CY, Cusack JC Jr, Liu R, Baldwin AS Jr. Control of inducible chemoresistance: enhanced anti-tumor therapy through increased apoptosis by inhibition of NF-kappaB. Nat Med 1999;5:412–7.
42. Campbell KJ, Rocha S, Perkins ND. Active repression of antiapoptotic gene expression by RelA(p65) NF-kappa B. Mol Cell 2004;13:853–65.